Impacts of biomass burning emissions and land use change on Amazonian atmospheric phosphorus cycling and deposition

Natalie M. Mahowald,[1] Paulo Artaxo,[2] Alex R. Baker,[3] Timothy D. Jickells,[3]
Gregory S. Okin,[4] James T. Randerson,[5] and Alan R. Townsend[6]

[1] Phosphorus (P) availability constrains both carbon uptake and loss in some of the world's most productive ecosystems. In some of these regions, atmospheric aerosols appear to be an important, if not dominant, source of new P inputs. For example, previous work suggests that mineral aerosols from North Africa bring significant amounts of new phosphorus to the P-impoverished soils of the Amazon Basin. Here we use recent observations and atmospheric transport modeling to show that the Amazon Basin itself appears to be losing atmospheric phosphorus to neighboring regions as a consequence of biomass burning emissions, anthropogenic sources of mineral aerosols and primary biogenic particles. Observations suggest that biomass burning emissions and human disturbance are responsible for ∼23% of the phosphorus flux in the Amazon. Although biomass burning and disturbance may bring new phosphorus into nondisturbed regions, as a whole the Amazon appears to be losing phosphorus through the atmosphere. Phosphorus lost via atmospheric transport from the Amazon is deposited in the adjacent oceans and in other regions downwind. These results suggest that land use change within the Amazon may substantially increase phosphorus availability to the remaining undisturbed forests, and that this fertilization mechanism could potentially contribute to recent changes in carbon uptake measured in undisturbed stands, as well as fertilizing downwind ocean regions.

Citation: Mahowald, N. M., P. Artaxo, A. R. Baker, T. D. Jickells, G. S. Okin, J. T. Randerson, and A. R. Townsend (2005), Impacts of biomass burning emissions and land use change on Amazonian atmospheric phosphorus cycling and deposition, *Global Biogeochem. Cycles*, *19*, GB4030, doi:10.1029/2005GB002541.

1. Introduction

[2] Tropical forests account for at least one-third of annual terrestrial biosphere-atmosphere carbon dioxide (CO_2) exchange [*Field et al.*, 1998], and therefore can modify climate and atmospheric composition at a global scale [e.g., *Dickinson and Henderson-Sellers*, 1988; *Shukla et al.*, 1990; *Townsend et al.*, 1992; *Malhi and Grace*, 2000; *Clark*, 2002]. In the Amazon basin, as in many of the world's lowland tropical regions, the majority of such forests are found on highly weathered soils (Ultisols and Oxisols) that contain low levels of available phosphorus (P) [*Sanchez et al.*, 1982; *Okin et al.*, 2004]. Evidence suggests that there is excess nitrogen in these same forests [*Martinelli et al.* 1999]. Thus, where nutrients limit primary productivity in tropical forests, it appears that phosphorus is the limiting nutrient for a large fraction of the world's lowland tropical regions [*Vitousek*, 1984; *Vitousek et al.*, 1988], although this may not be true of all moist tropical forests [*Lloyd et al.*, 2001]. The widespread distribution of low-P soils in tropical latitudes has, in turn, caused atmospheric inputs of aerosol-bound phosphorus to be linked with the long-term productivity of these forests [e.g., *Swap et al.*, 1992; *Chadwick et al.*, 1999; *Wardle et al.*, 2004].

[3] Atmospheric phosphorus exists almost entirely in the form of aerosols due to the low volatility of phosphorus compounds. Reviews of atmospheric phosphorus provide evidence for the dominance of mineral aerosols in delivering atmospheric phosphorus to oceans and other ecosystems on a globally averaged basis [*Graham and Duce*, 1979, 1982]. Although atmospheric inputs of phosphorus in mineral aerosols are typically quite low for most ecosystems, they are thought to be an important source of new phosphorus to moist tropical forests on geologic timescales [*Swap et al.*, 1992; *Chadwick et al.*,

---

[1]National Center for Atmospheric Research, Boulder, Colorado, USA.

[2]Instituto de Fisca, Universidade de Sao Paulo, Sao Paulo, Brazil.

[3]School of Environmental Sciences, University of East Anglia, Norwich, UK.

[4]Department of Environmental Sciences, University of Virginia, Charlottesville, Virginia, USA.

[5]Earth System Science Department, University of California, Irvine, California, USA.

[6]Department of Ecology and Evolutionary Biology and Institute of Arctic and Alpine Research, University of Colorado, Boulder, Colorado, USA.
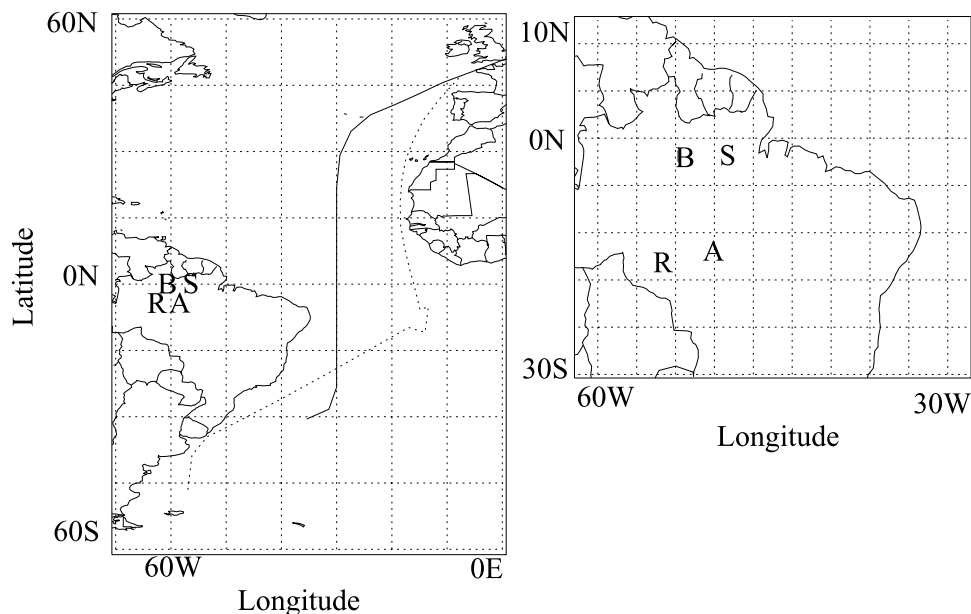
Figure 1. Locations of the observations used in this paper. The cruise track for the *Polarstern* cruise [*Losno et al.*, 1992] is the solid line and the measurements were taken between 14 September and 5 October 1988. The cruise track for the *James Clark Ross* [*Baker et al.*, 2003, 2005] is the dashed line and the observations were taken between 10 September and 24 October 2001. Alta Floresta (A) is at 10°S, 57°W, Balbina (B) is at 2°S, 60°W, Rondonia (R) is at 11°S, 62°W, and Santarem (S) is at 2°S, 55°W.

1999; *Okin et al.*, 2004]. However, while mineral inputs may well be important at long timescales, recent observations over tropical forest regions do not support the dominance of mineral aerosols for the atmospheric phosphorus cycle in these areas. Primary biogenic particles (which are not well understood, but will likely include spores, pollen, leaf fragments, and dead microorganisms) appear to contribute substantially to atmospheric phosphorus over the Amazon [*Artaxo et al.*, 1988; *Graham et al.*, 2003]. Additionally, recent observations have highlighted the role of biomass burning as a source of atmospheric phosphorus in tropical savanna and forests [*Echalar et al.*, 1995; *Ferek et al.*, 1998; *Gaudichet et al.*, 1995; *Reid et al.*, 1998; *Turn et al.*, 1997], although some studies do not show elevated values of phosphorus in biomass burning plumes [*Cachier et al.*, 1995; *Maenhaut et al.*, 1996].

[4] In this paper we assess the contribution of biomass burning, mineral, and biogenic sources of atmospheric phosphorus fluxes within the Amazon basin using observations from the Amazon basin and atmospheric modeling. As part of our analysis, we examine the role of humans in perturbing the atmospheric phosphorus cycle, a topic that has not been addressed in previous studies. In section 2 we present methods for the paper, including a description of the observations, analyses of observations, and the model that we use in the paper. In section 3 we present the results of the analysis of the observations and comparisons of the model to observations, which allow us to extrapolate the observations to the basin as a whole. In section 4 we examine the biogeochemical implications of

the changing atmospheric phosphorus cycle and summarize the results of this paper.

2. Methodology

2.1. Description of Observations

[5] Aerosol samples at Alta Floresta (10°S, 57°W), Balbina (2°S, 60°W), Rondonia (11°S, 62°W) and Santarem (2°S, 55°W) stations in the Amazon were collected over several months to years as part of the Large Scale Biosphere Atmosphere Experiment in Amazonia (LBA). The aerosol sampling and analysis techniques were described in some detail by *Artaxo et al.* [2002], and are only briefly described here. The locations of the sampling sites are shown in Figure 1. Aerosol samples were collected for the fine mode fraction (diameter < 2.0 μm) using a Nuclepore 0.4 μm pore size filter, and for coarse mode (2.0 < diameter < 10.0 μm) using a Nuclepore 8 μm pore size filter. Sampling times were typically 24 to 48 hours. Elemental analysis was conducted using Particle-Induced X-Ray Emission (PIXE) analysis and concentrations of up to 21 elements (Mg, Al, Si, P, S, Cl, K, Ca, Ti, V, Cr, Mn, Fe, Ni, Cu, Zn, Br, Rb, Sr, Zr, and Pb) were obtained (details are given by *Artaxo and Orsini* [1987], *Johansson et al.* [1995], and *Artaxo et al.* [2002]. Detection limits were typically 5 ng m^{-3} for elements in the range 13 < Z < 22 and 0.4 ng m^{-3} for elements with Z > 22. Precision of elemental concentration measurements was typically better than 7%, reaching up to 20% for values near the detection limit. Blank values were obtained analyzing at least 20 field blank filters for each sited transported together with the real samples. Black

carbon concentrations were obtained by a light reflectance technique [*Martins et al.*, 1998a, 1998b].

[6] Alta Floresta had 205 daily averaged values during 1996–1998; 150 of the measurements in the coarse mode and 131 in the fine mode had detectable levels of phosphorus. Balbina had 345 coarse and 304 fine daily averaged values during 1998–2002, all of which had detectable values for phosphorus. Rondonia had 87 daily averaged values during September–November of 2002; 87 of these in the coarse mode, and 16 of these in the fine mode had detectable levels of phosphorus. Santarem had 290 daily averaged values during 2000–2002; 290 of these measurements in the coarse mode, and 248 of these in the fine mode had detectable levels of phosphorus. Phosphorus is a particularly difficult element to measure at $1–50$ ng m^{-3}; filter blank values for phosphorus were negligible.

[7] Aerosol samples were also collected over the Atlantic Ocean during cruises of RV *Polarstern* (14 September to 6 October 1988) [*Losno et al.*, 1992] and RRS *James Clark Ross* (JCR, 10 September to 24 October 2001) [*Baker et al.*, 2003]. Bulk aerosol was collected during the *Polarstern* cruise and concentrations of P, K, Al and other elements was determined by wavelength dispersive X-ray fluorescence spectrometry (CGD alpha 10) as described by *Losno et al.* [1992]. Reported uncertainties of these measurements are less than 7%. During the JCR cruise two high volume (1 m^3 min^{-1}) collectors equipped with cascade impactors for aerosol size segregation (coarse/fine split at 1 μm) were used to collect paired samples for trace metal (TM) and major ion (MI) analysis. Aerosol collection substrates were all Whatman 41 paper. Substrates used for TM sampling were acid-washed before use, while MI substrates were used without any pretreatment. Total Al and P were extracted from fractions of the TM aerosol samples by strong acid (HNO$_3$/HF) digestion and subsequent determination by Inductively Coupled Plasma–Optical Emission Spectrometry (Al) and High Resolution magnetic sector Inductively Coupled Plasma–Mass Spectrometry (P). Soluble ions (including Na$^+$ and K$^+$) were determined by ion chromatography after extraction of a quarter of the MI filters in ultrapure water. Full analytical details for all these procedures can be found elsewhere [*Baker et al.*, 2005]. Na$^+$ data were used to calculate the component of aerosol K$^+$ concentrations arising from non-seasalt (nss K) sources by assuming that aerosol Na$^+$ was derived exclusively from seaspray [see *Baker*, 2004]. See Figure 1 for the location of these cruise observations.

[8] The observations are analyzed using several statistical techniques. Simple correlations and regressions are used for most of the paper, due to the simplicity of interpreting the results. In order to verify that our results are not sensitive to this approach, we also show results using multicomponent regressions, where we regress the phosphorus onto aluminum, black carbon and potassium, and determine the slopes simultaneously. Finally, we use principal component analysis to determine the leading principal components, using the methodology of *Artaxo et al.* [1998] (see that paper for more details and references). In principal component analysis, one models the variability of the observations, so that orthogonal sets of intercorrelated variables is found. This is

found by finding the eigenvectors and eigenvalues of the correlation matrix. Then the most important eigenvectors are rotated using a VARIMAX rotation to maximize the variability in the eigenvectors, resulting in groups of elements that tend to vary together (called "factors"). Only eigenvectors with an eigenvalue above 1.0 are included in the rotation. Factor loadings are calculated, which represent the correlation between the observed element time series and the time series of each factor as determined from the VARIMAX rotation. Principal component analysis results are very sensitive to which elements are included; we include the following elements that were measured at the sites (BC, Mg, Al, Si, P, S, Cl, K, Ca, Ti, V, Cr, Mn, Fe, Cu, Zn, Br, Pb), All the statistical methods used in this paper are based on a correlation analysis, so we expect similar results.

2.2. Model Description

[9] Sources, transport and deposition of phosphorus in aerosols are calculated using the Model of Atmospheric Transport and Chemistry (MATCH) [*Rasch et al.*, 1997; *Mahowald et al.*, 1997] with National Center for Environmental Prediction/National Center for Atmospheric Research (NCEP/NCAR) reanalysis winds [*Kistler et al.*, 2001] for 2000 to simulate dust, biomass burning and primary biogenic aerosols. MATCH is an example of an offline chemical transport model, which uses meteorological winds from a forecast center to solve the mass conservation equations in three-dimensional space globally using a time step of 40 min. The MATCH model uses the resolution of the input data set, which in this case is T62 (1.8° by 1.8°) with 26 vertical levels. Simulations start on 1 December 1999 and end 31 December 2000, with the first month considered spinup and not used for the analysis. Because of the short lifetime of the constituents considered (<2 weeks), a one month spin up is sufficient. For each grid box, we obtain a concentration, as well as an estimate of both the wet and dry deposition fluxes from that grid box for every day of the year, explicitly incorporating seasonality into the simulation.

[10] Desert dust is modeled following *Mahowald et al.* [2002, 2003] and *Luo et al.* [2003] using the Dust Entrainment and Deposition module [*Zender et al.*, 2003]. Model results have been extensively compared with observations [*Mahowald et al.*, 2002, 2003; *Luo et al.*, 2003]. The source of mineral aerosols is dry, unvegetated regions with easily erodible soils and high winds, and it will vary on diurnal, synoptic and seasonal timescales. We use the *Ginoux et al.* [2001] map of unvegetated regions with easily erodible soils, and a dust entrainment mechanism based on wind tunnel studies [*Zender et al.*, 2003; *Iversen and White*, 1982; *Marticorena and Bergametti*, 1995; *Gillette et al.*, 1997; *Fecan et al.*, 1999]. Dry deposition processes include both turbulent and gravitational settling following *Seinfeld and Pandis* [1996]. Wet deposition assumes a simple scavenging ratio during precipitation events [*Mahowald et al.*, 2002]. Once the aerosols are entrained into the atmosphere, they undergo transport, wet and turbulent dry deposition and gravitational settling appropriate for their assumed composition and size. Phosphorus is assumed to be

700 μg/g of mineral aerosols [*Chadwick et al.*, 1999]. We do not attempt to capture the locally produced dust seen in the observations at Alta Floresta (that we infer from high Al concentrations), because we do not know over how large an area these same high concentrations are seen.

[11] Fine mode biomass burning aerosols use the methodology following *Rasch et al.* [2001], with the monthly mean biomass burning source from *van der Werf et al.* [2003]. Emissions were doubled to match the means of the fine mode black carbon observations at the four Amazon sampling stations. We assume the phosphorus is associated with the organic carbon aerosols, which are treated as originally hydrophobic, and converting to hydrophilic on a 1.5-day e-folding timescale (e-folding timescale is one over the first order rate constant or the time over which the constituent will be reduced to e^{-1} of its original magnitude). Turbulent dry deposition and wet deposition act as loss mechanisms from the atmosphere for fine particles. To match the observations, coarse mode biomass burning aerosols are assumed to have a source that is 20% of the fine mode source. Coarse mode biomass burning aerosols are modeled similar to the coarse mode desert dust aerosols using two size bins (2.5–5 and 5–10 μm), and modeled to gravitationally settle out of the atmosphere, in addition to turbulent dry and wet deposition processes. Phosphorus is assumed to be emitted in the model with a ratio of P/BC in fine mode of 0.0029 and P/BC in coarse mode of 0.02, based on slope using all the observations (Table 1 and section 3.1).

[12] To simulate primary biogenic aerosols, we assume that primary biogenic aerosol emissions are spatially proportional to annually averaged above ground biomass from *van der Werf et al.* [2003] with a constant source year round. To obtain the magnitude of the source, we match the observed ratio of phosphorus from biomass burning divided by phosphorus from biogenic particles (using the means from all four stations). This results in an emission factor of $8.9e^{-18}$ gP g above ground C^{-1} s^{-1}. Deposition processes for the primary biogenic particles are calculated similar to the coarse mode desert dust aerosols using two size bins (2.5–5 and 5–10 μm), and include turbulent and gravitational dry deposition as well as wet deposition during precipitation events.

[13] These model assumptions are necessarily crude, but represent the first attempts to model atmospheric phosphorus. As described above, where possible we used the observations to constrain the model simulations.

3. Analysis of Atmospheric Phosphorus in the Observations and Model

3.1. Observed Atmospheric Phosphorus Results

[14] Figure 2 shows the monthly mean observed phosphorus values at Alta Floresta [*Artaxo et al.*, 2002], Balbina, Rondonia and Santerem, as well as the aluminum concentrations (2e) and precipitation (2f) at each station (precipitation from *Chen et al.* [2002]). Mean values of the observed concentrations of selected components and their correlation with phosphorus are shown in Table 1. Mean concentrations of phosphorus range from 34 to 102 ng m^{-3}

over the sampling stations, with most of the phosphorus in the coarse mode. Across all four stations, we observe statistically significant correlations in the fine mode between phosphorus and biomass burning aerosols (BC and potassium, which both indicate biomass burning in the fine mode [*Andreae*, 1983]), and in the coarse mode between phosphorus and potassium (Table 1). We interpret the high correlations between phosphorus and biomass burning aerosols (BC and potassium in the fine mode) as evidence that biomass burning represents a source of phosphorus to the atmosphere [*Gaudichet et al.*, 1995; *Maenhaut et al.*, 1996; *Andreae et al.*, 1998]. If we use the data at these stations to estimate an emission ratio of phosphorus relative to black carbon from biomass burning, we obtain a mass ratio of 0.0029 ± 0.0001 P/BC in the fine mode and 0.0191 ± 0.004 P/BC in the coarse mode. In previous studies, similar ratios were seen in biomass burning plumes in Africa and South America [*Echalar et al.*, 1995; *Ferek et al.*, 1998; *Reid et al.*, 1998], although some studies did not observe higher phosphorus in biomass burning plumes [*Cachier et al.*, 1995; *Maenhaut et al.*, 1996]. These values represent approximately 1.5–10 μg P emitted per g C burned (using black carbon emission factors from [*Andreae and Merlet*, 2001]), a range considerably smaller than the original plant material ratios of 600 μg P g C^{-1} [*McGroddy et al.*, 2004].

[15] At all four stations, there is no significant correlation between aluminum (a proxy for mineral aerosols) and phosphorus, although when all four stations are combined, a low but statistically significant correlation is found (Table 1). If we assume that phosphorus has a mass concentration of 700 μg P g^{-1} in mineral aerosols and that aluminum comprises 7% of mineral aerosols [e.g., *Okin et al.*, 2004], then the phosphorus in mineral aerosols observed in Brazil represents only between 2% and 29% of the total measured phosphorus (shown as phosphorus derived from mineral aerosols in Table 1). Two lines of evidence suggest that the mineral aerosols at Alta Floresta and Rondonia originate primarily from sources in South America, and do not represent long-range transport of mineral aerosols from North Africa. First, the highest aluminum measurements are at Alta Floresta, despite this site being farther from the North Africa mineral aerosol sources than the other observation stations (Figure 2e; station locations are shown graphically in Figure 1). Model results support that concentrations of North African dust should be lower at Alta Floresta than at Balbina (see section 3.2). Second, the aluminum measurements at Alta Floresta and Rondonia reach a maximum during the dry season (July-August, Figures 2e and 2f), which is not when North African mineral aerosol transport to South America is highest, as seen at Balbina and Santarem in Figure 2e (see discussion and Figures 4c, 5c, 6c, and 7c in section 3.2). It is likely that the Alta Floresta aluminum comes from local sources, including mineral aerosols entrained into biomass burning plumes as a result of strong convection and dry soils near the flaming front [*Gaudichet et al.*, 1995]. Another alternative is that the aluminum (and therefore the phosphorus) comes from industrial sources. However, because of the lack of industry near these observing stations, it is unlikely that the aluminum comes from industrial sources. We can

Table 1. Estimate of Phosphorus Aerosol Sources at Four Brazilian Stations[a]

Constituent	Fine Concentration, ng m^{-3}	Coarse Concentration, ng m^{-3}	Fine Correlation[b]	Coarse Correlation[b]	Fine Slope[c]	Coarse Slope[c]	Component Contribution to Fine P, n[d]	Component Contribution to Coarse P[d]	% Fine P, Contribution/ Observed	% Coarse P, Contribution/ Observed	% Total P, Contribution/ Observed
Alta Floresta											
P	20	82									
Al (mineral aerosols)	501	2460	0.29	NS	0.0068	NS	5.0	24.6	25	30	29
BC (biomass burning)	6170	1660	0.80	NS	0.0025	NS	17.9	33.2	88	40	50
K (biogenic particles)[d]	1020	373	0.80	0.37	0.0159	0.0724	0.0	51.3	0	62	50
Balbina											
P	5	30									
Al (mineral aerosols)	50	74	NS	NS	NS	NS	0.5	0.7	10	2	4
BC (biomass burning)	325	56	0.40	NS	0.0040	NS	0.9	1.1	19	4	6
K (biogenic particles)[d]	91	89	0.56	0.61	0.0171	0.1869	0.0	12.2	0	41	35
Rondonia											
P	5	25									
Al (mineral aerosols)	90	225	0.76	NS	0.0363	NS	0.9	2.3	19	9	11
BC (biomass burning)	2040	149	0.65	0.23	0.0010	0.0324	5.9	3.0	126	12	30
K (biogenic particles)[d]	461	119	0.66	0.51	0.0053	0.1143	0.0	16.5	0	67	56
Santarem											
P	4	64									
Al (mineral aerosols)	46	77	0.33	NS	0.0079	NS	0.5	0.8	12	1	2
BC (biomass burning)	524	124	0.65	0.36	0.0034	0.3056	1.5	2.5	38	4	6
K (biogenic particles)[d]	138	138	0.73	0.89	0.0130	0.4213	0.0	18.9	0	30	28
Total[e]											
P	7	50									
Al (mineral aerosols)	171	652	0.48	0.20	0.0129	0.0070	1.7	6.5	23	13	14
BC (biomass burning)	1906	129	0.85	0.20	0.0029	0.0191	5.5	2.6	74	5	14
K (biogenic particles)[d]	358	178	0.85	0.58	0.0184	0.1375	0.0	24.4	0	49	43

[a]Aluminum (Al), a proxy for mineral aerosols; black carbon (BC), a proxy for biomass burning; and potassium (K), a proxy for biogenic particles in the coarse mode.

[b]Correlation between P concentrations and indicated constituent over all data at the station. Only statistically significant values at the 95% are shown in the table (NS indicates not significant).

[c]Slope calculated doing a regression between P and indicated constituent over all data at the station. Values are only shown when correlation coefficient is statistically significant (NS indicates not significant), and the values are statistically significantly different than zero.

[d]Contributions are calculated on the basis of mean concentrations observed at the station and the following P ratios: For Al in fine or coarse mode, use continental values of 7% Al and 0.07% P. For BC, use observed slopes of 0.0029 for fine and 0.02 for coarse mode. For K, use observed slope of 0.1375 for coarse mode (assuming that fine mode K is from biomass burning).

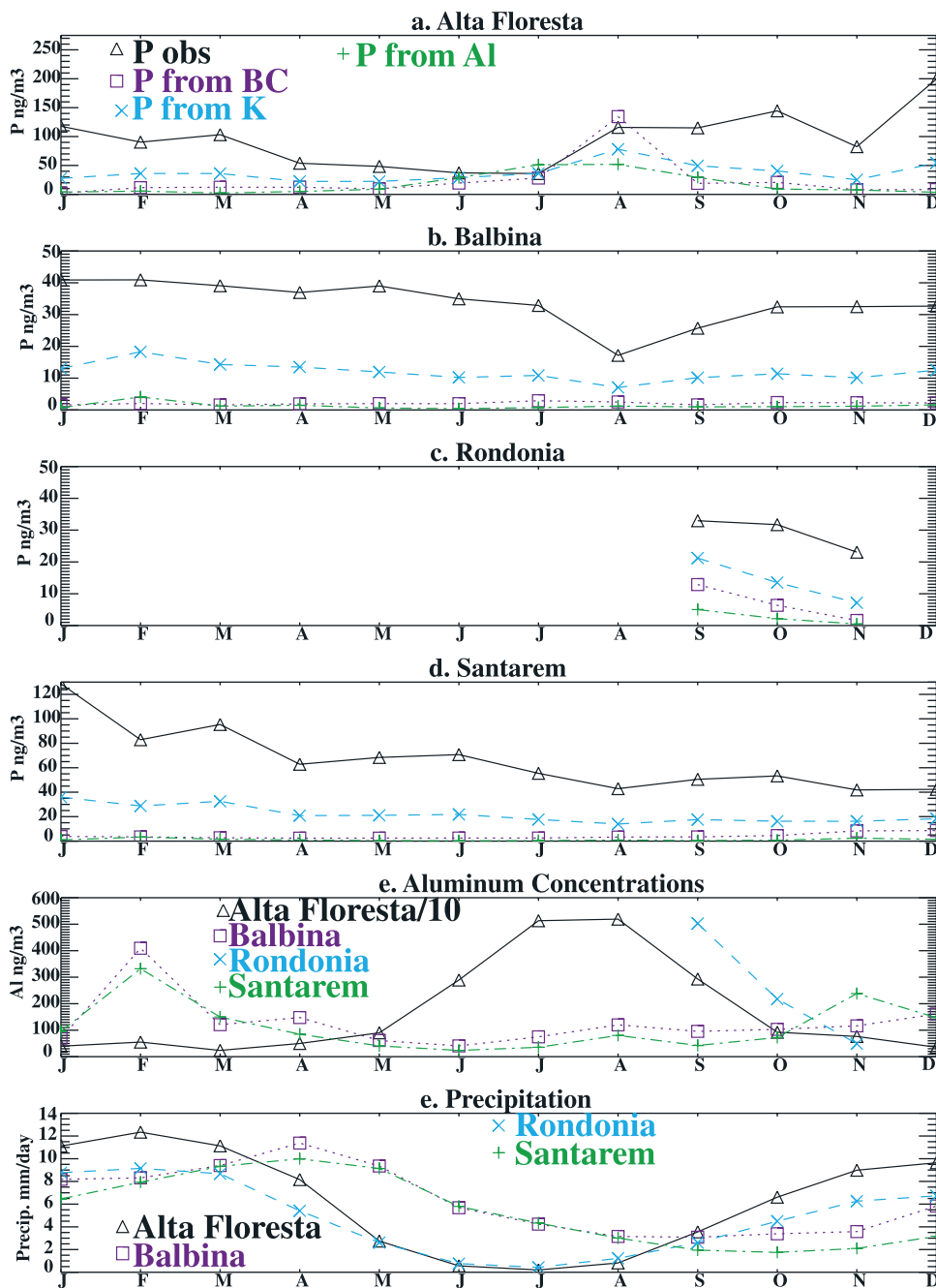[e]Estimates made over data from all four stations simultaneously.

Figure 2. Monthly averaged observations of Phosphorus (P obs), and the estimated contribution to the observed phosphorus from observations of biomass burning (P derived from BC), biogenic aerosols (P derived from K), mineral aerosols (P derived from Al), and the total of these estimated sources of phosphorus (P est). Also included are the model results for phosphorus based on the atmospheric transport model and emission sources described in the sections 2.2 and 3.2. Estimations of phosphorus use the following relationships: P/BC in fine mode is 0.0029, P/BC in coarse mode is 0.02, P/Al is 0.01, and P/K is 0.1375, as described in more detail in the text. Figure 2e shows aluminum concentrations (ng/m^3) at each of the four stations. Please note that the aluminum concentrations at Alta Floresta are divided by 10.0 in order to fit on the same figure with the other observational sites. Figure 2f shows monthly averaged gridded precipitation (mm/day) for each of the four stations averaged over 1980–1999 from *Chen et al.* [2002].

use enrichment factors (Al/Fe in the aerosol over Al/Fe in crustal materials) to verify this [*Pye*, 1987]. The median Al/Fe and Al/Si ratios in these samples are 1.4 and 0.66, respectively, while crustal values are 1.6 and 0.3 [*Mason and Moore*, 1984], giving us enrichment factors of 0.88 and 2.2, respectively. Normally, enrichment factors above 10.0 indicate a substantial anthropogenic source of material [*Pye*, 1987]; thus these values suggest a crustal source for the aluminum.

[16] Although biomass burning accounts for almost all of the phosphorus in the fine mode, it accounts for only a small part of the phosphorus in the coarse mode (Table 1). Other processes must be invoked to explain the remainder of phosphorus in the coarse mode and thus the majority of phosphorus mass in the atmosphere (Table 1). Coarse mode aerosols are usually emitted directly (called primary aerosols) and not formed in the atmosphere from condensation processes. A tracer of primary biogenic aerosols, coarse mode potassium (K) [*Artaxo and Maenhaut*, 1990], shows a moderate correlation in the coarse mode for all the sites, suggesting that the remainder of the phosphorus may be associated with primary biogenic aerosols. Previous studies [*Artaxo et al.*, 2002; *Graham et al.*, 2003] suggest that the variability in the coarse mode phosphorus during day and nighttime is consistent with these particles being part of natural ecosystem phosphorus cycling. Both observed phosphorus and coarse mode potassium have smaller and different seasonal cycles than biomass burning (BC) or aluminum We can see this in Figure 2, where the observed phosphorus has almost no strong peak (except for a modest peak at Santarem in January), while the biomass burning or aluminum maximum is quite distinct and can be a factor of 10 higher than the concentration during other months. On the other hand, the potassium also has a weak seasonal cycle (Figure 2; see section 3.2 for more discussion). Using the observed P/K ratios (0.1375 ± 0.0066 g P/g K in the coarse mode), primary biogenic aerosols are responsible for 28–56% of the total observed phosphorus (Table 1). Table 1 and Figure 2 (and discussion in section 3.2) show that estimating the phosphorus from the aluminum, black carbon and potassium does not capture all the variability in the phosphorus data, but does seem broadly consistent with the seasonal cycle in phosphorus directly observed. The particle types of the primary biogenic aerosols is not well established, but will include spores, pollen, leaf fragments, and dead microorganisms and have been speculated to be a large fraction of the total aerosol mass over tropical forests [*Penner et al.*, 2001; *Graham et al.*, 2003].

[17] To verify that our results are robust to different statistical analyses, we conduct multicomponent regressions of P against Al, BC and K together. In this case we obtain slopes of -0.00004 ± 0.007, 0.0011 ± 0.0004 and 0.011 ± 0.003 in the fine mode and 0.0052 ± 0.0022, -0.099 ± 0.0056 and 0.31 ± 0.011 in the coarse mode for Al, BC, and K, respectively. It is difficult to interpret negative slopes in this case, but they are consistent with a low percentage of the P associated with Al in the fine mode and BC in the coarse mode, as suggested in Table 1. These results are also consistent with fine mode P being associated with black carbon and potassium, and coarse mode P being associated

with aluminum and potassium, which we see in the correlations and contributions in Table 1. The slopes from the multicomponent regression are not the same as we use in Table 1, and because of the negative slopes for some components, we chose to use the single regression slopes for the analysis in the rest of the paper (Table 1).

[18] Principal component analysis identifies the elements of the aerosol analysis that vary together by identifying a reduced number of elemental combinations that describe most of the variability in the aerosol samples. Principal component analysis (also called absolute principal factor analysis or empirical orthogonal functions) has been used in previous studies to determine source apportionment, instead of the more simple correlations used here [e.g., *Artaxo et al.*, 1998]. First, the principal components are determined with their eigenvalues, and then the eigenvectors with an eigenvalue above a value of 1.0 (containing most of the variability) are retained, and the eigenvectors are rotated to maximize the variability. In many cases, this separates out the elements more easily. For the fine mode, the first seven eigenvalues are 9.6, 1.7, 1.5, 1.3, 0.95 and 0.87. We chose to show results from the first four eigenvalues rotated, taking the eigenvectors with values above 1.0 similar to previous analyses [e.g., *Artaxo et al.*, 1998]. The results of the VARIMAX rotated principal components are shown in Table 2 as "loadings," which represent the correlation between the observed time series for each element and the time series for the factors. Unfortunately, in our case, there is not a clear separation between different types of aerosols. All factors appear to have a moderate to strong correlation with black carbon. But the factor with the strongest correlation with black carbon (factor 1), also has the strongest correlation with phosphorus, which strongly implicates biomass burning as a source of phosphorus, consistent with our results from Table 1 for fine particles. For the coarse mode, the eigenvalues from the principal component analysis are 9.1, 2.6, 2.0, 1.7, 1.2, 0.95 and 0.88. We chose to show results from the rotation of five eigenvectors in Table 3, again keeping eigenvectors which correspond to eigenvalues above 1.0. Again, there is not a clear separation of different aerosol types, with most factors have moderate to strong correlations between black carbon and aluminum and potassium. The highest correlation for phosphorus is with the factor 4, which has the highest correlations with potassium and sulfur (indicators of biogenic particles). It also has moderate to high correlations with black carbon (indicative of biomass burning), magnesium and calcium (indicative of biogenics) and aluminum, silica and iron (indicative of soil particles). Overall the principal component analysis does not give us a clear picture of the source apportionment, similar to some previous studies [e.g., *Reid et al.*, 1998], but the results of the principal component analysis are qualitatively consistent with the results of the simple correlations shown in Table 1.

[19] To understand whether the observations of high atmospheric phosphorus in the Amazon are representative of a larger region, we looked for observations in other tropical regions. Results from two cruises in the Atlantic during the September-October time period [*Losno et al.*, 1992; *Baker et al.*, 2003, 2005] show that there are elevated

Table 2. Factor Loadings for Fine Aerosols

Element	Factor 1	Factor 2	Factor 3	Factor 4
BC	−0.95	−0.52	0.37	0.60
MG	−0.84	−0.64	0.81	0.65
AL	−0.55	−0.98	0.18	0.45
SI	−0.49	−0.94	0.20	0.37
P	−0.92	−0.47	−0.21	0.71
S	−0.85	−0.38	0.32	0.63
CL	−0.89	−0.42	0.30	0.70
K	−0.97	−0.51	0.34	0.54
CA	−0.25	−0.01	−0.11	−0.48
TI	−0.57	−0.97	0.23	0.49
V	−0.22	−0.71	0.08	0.25
CR	−0.61	−0.39	0.97	0.67
MN	−0.68	−0.89	0.29	0.48
FE	−0.58	−0.97	0.19	0.36
CU	−0.74	−0.48	0.27	0.54
ZN	−0.91	−0.55	0.33	0.71
BR	−0.79	−0.38	0.33	0.94
PB	−0.43	−0.23	−0.05	0.96

phosphorus concentrations south of the equator in the Atlantic (Figure 3). In the southern tropical Atlantic, substantial levels of phosphorus cannot be explained by mineral aerosols (Al), but are related to higher non-sea-salt potassium (K) [*Losno et al.*, 1992] (also seen in data from *Baker et al.* [2003, 2005], not shown). Most of the phosphorus is in aerosols with a radius greater than 1 μm during the 2001 cruise [*Baker et al.*, 2005] (no size data are available for the other cruise), consistent with coarse primary biogenic or biomass burning aerosols being an important source of phosphorus in the tropical South Atlantic. Because these cruises are not downwind of the Amazon during this time period (according to model calculations discussed in more detail in section 3.2), these data appear to support not just the Amazon, but tropical terrestrial biomass and biomass burning in general being a source of atmospheric phosphorus.

3.2. Model/Data Comparisons

[20] To make phosphorus budget for the entire Amazonian basin, we need to extrapolate the available observations

Table 3. Factor Loadings for Coarse Aerosols

	Factor 1	Factor 2	Factor 3	Factor 4	Factor 5
BC	−0.65	0.67	0.19	−0.82	0.44
MG	−0.69	0.24	0.52	−0.49	0.95
AL	−0.96	0.54	0.35	−0.48	0.30
SI	−0.98	0.54	0.38	−0.51	0.40
P	−0.17	−0.14	0.16	−0.68	0.05
S	−0.41	0.35	0.52	−0.91	0.66
CL	−0.12	0.06	0.92	−0.21	0.35
K	−0.65	0.40	0.42	−0.91	0.46
CA	−0.75	0.29	0.50	−0.59	0.59
TI	−0.99	0.56	0.33	−0.48	0.37
V	−0.93	0.76	0.49	−0.35	0.22
CR	0.02	0.98	0.02	0.05	0.08
MN	−0.94	0.47	0.36	−0.56	0.47
FE	−0.98	0.55	0.33	−0.48	0.35
CU	−0.11	0.02	0.93	−0.10	−0.01
ZN	−0.29	0.15	0.06	−0.38	0.19
BR	−0.47	0.06	0.05	−0.17	0.64
PB	−0.56	0.09	−0.13	−0.42	−0.20

using a model. Additionally, model results allow us to test our hypothesis in a consistent manner. Figures 4–7 show the monthly mean aerosol concentrations from the observations and the model predictions. Notice that at Alta Floresta and Santarem there are distinct biomass burning seasons, and they occur at different times of the year at these different locations, associated with the different rainfall seasonality (Figure 2f). The Rondonia data was only collected during the biomass burning season, while the Balbina observations show less black carbon (600 ng m^{-3} compared with 3500 ng m^{-3} for Alta Floresta), but the black carbon is observed during much of the year. The model appears to capture the maximum months for biomass burning at Alta Floresta and Santarem, but misses the indistinct peak for Balbina. Model values were doubled to best match the mean observations, but the modeled BC concentrations are too low at Alta Floresta and Balbina and too high at Rondonia.

[21] The fine mode potassium at Alta Floresta, Balbina and Santarem has a seasonal cycle similar to the black carbon (BC), consistent with fine mode potassium (K) coming from biomass burning. However, the coarse mode potassium has a much smaller seasonality than the fine mode (e.g., at Alta Floresta fine BC concentrations are 20× higher in August than January, while coarse potassium concentrations are 2× higher) and appears to have a maximum in a different month at Alta Floresta, Balbina and Santarem, This is consistent with the potassium being from primary biogenic aerosols in the coarse mode. Observations suggest that most potassium from biomass burning
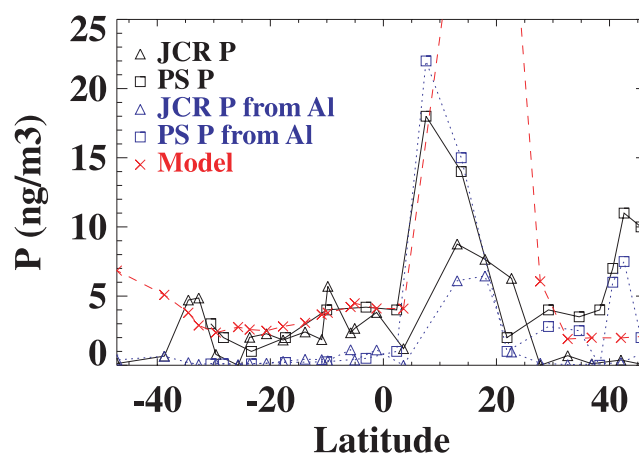

Figure 3. Atlantic data from the *Polarstern* (PS) and *James Clark Ross* (JCR) cruises show the observed phosphorus concentrations [*Losno et al.*, 1992; *Baker et al.*, 2003, 2005] and the inferred amount of phosphorus in mineral aerosols (assuming that phosphorus is 700 μg g^{-1} of mineral aerosols, and aluminum is 7% of mineral aerosols by mass) (P derived from Al in the figure legend). Modeled results are also shown (section 3.2). Note that model results shown similar peaks and troughs, although the mineral aerosol component of phosphorus appears to be overestimated in model between 10°N and 25°N and south of 35°N [*Hand et al.*, 2004]. Figure 1 shows the locations of the cruise observations.
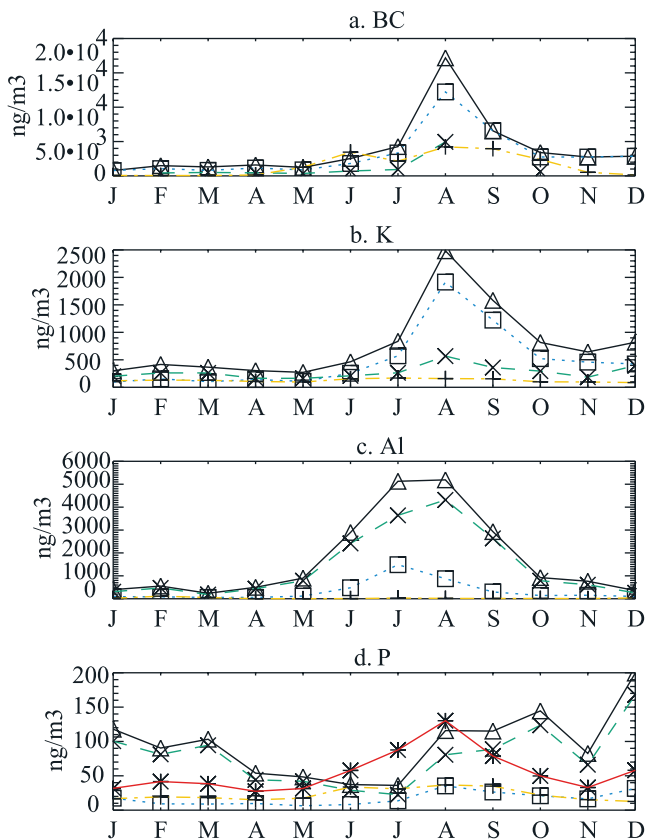
Figure 4. Monthly averaged aerosol concentrations (μg m⁻³) at the Alta Floresta for black carbon (BC), potassium (K), aluminum (Al) and phosphorus (P). Black lines (triangles) are the observational totals, while the dark blue lines (squares) are the fine fraction in the observations and the green lines (crosses) are the coarse fraction. Model predictions are shown in yellow/orange (pluses), and in the phosphorus plot, the red line (asterisks) shows the estimated phosphorus using observations and the following ratios: P/BC fine = 0.0019, P/BC coarse = 0.02, P/Al = 0.01, P/K coarse = 0.1375, P/K fine = 0. BC represents biomass burning aerosols, Al represents mineral aerosol and coarse K represents primary biogenic aerosols, in this analysis.

is in the fine mode [*Gaudichet et al.*, 1995; *Maenhaut et al.*, 1996; *Andreae et al.*, 1998]. The modeled potassium from primary biogenic aerosols should be compared to the coarse potassium in the observations, and is too low at Alta Floresta, too high at Balbina and roughly similar at the other two stations. The modeled primary biogenic aerosol has no seasonal cycle in the emissions, and this simple assumption does not seem obviously wrong from the comparison with the coarse potassium observations.

[22] Observations of aluminum show that at Balbina and Santarem the peak is in November-February, and the model captures this seasonality, although the model overestimates the aluminum by a factor of 2. In the model, all this aluminum comes from North Africa, since it is the closest dust source. At Alta Floresta and Rondonia we see higher

aluminum than at Balbina or Santarem during the biomass burning season, which appears to be associated with local dust sources or biomass burning [*Gaudichet et al.*, 1995] as discussed in section 3.1. Alta Floresta and Rondonia are farther downwind from North Africa than Balbina and Santarem and have much lower dust concentrations during November to February time frame when the North Africa dust is transported to this region (see Figure 2e).

[23] The final panel for each station shows the observed phosphorus in all months is dominated by the coarse mode. While the phosphorus appears elevated during the biomass burning seasons (months with elevated BC), the highest phosphorus appears after the biomass burning seasons at Santarem and Alta Floresta. Note that at Santarem the highest concentrations occur in January, while the lowest occur in December, an unusual seasonal cycle that could be the result of only 2 years of data collected at these sites.

[24] These model results suggest that the simple modeling of phosphorus cycling the Amazon captures the important features of the observed phosphorus, but that future studies could improve the modeling. The model tends to under-predict phosphorus by about a factor of 2, but given the uncertainties in the phosphorus budget, we can use the model results to look at the budget of atmospheric phosphorus more closely in section 4.
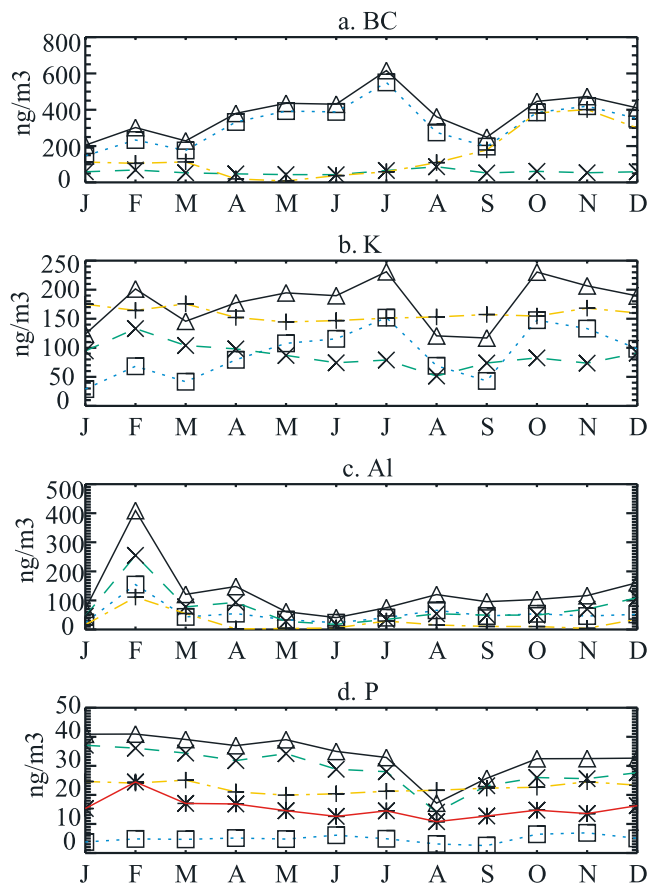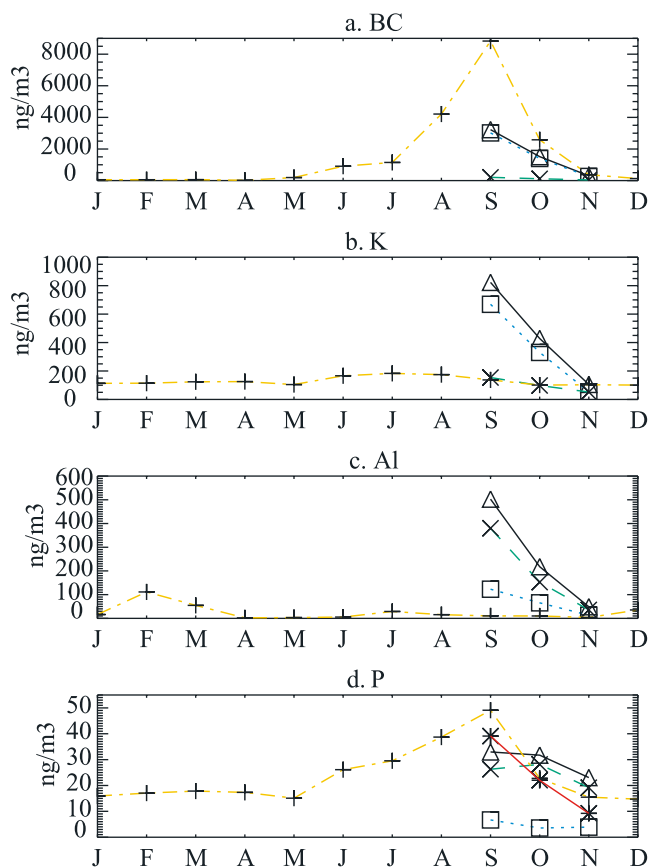

Figure 5. Same as Figure 4 but for Balbina.

Figure 6. Same as Figure 4 but for Rondonia.

Hawaii clearly shows the importance of atmospheric phosphorus to the fertility of older, P-poor soils [*Chadwick et al.*, 1999]. Thus the net balance between long-range transport of mineral aerosols and local sources of atmospheric phosphorus into the atmosphere, from both biogenic aerosols and human disturbance, is likely to be important to the structure and function of many Amazonian ecosystems.

[27] The results described in section 3.1 suggest that even in the absence of significant human disturbance, combustion and biogenic sources of atmospheric phosphorus within the Amazon may contribute to atmospheric phosphorus deposition more than long-range transport of mineral aerosols. Thus, prior to the expansion of agriculture and deforestation within the Basin, variations in the phosphorus fertility of Amazonian forests may have developed not only due to changes in parent material and soil type, but also to gradients in the balance between these potential inputs and losses of atmospheric phosphorus.

[28] More recently, widespread deforestation, logging, and human settlement within the Amazon appear to be causing substantial changes in the exchange of phosphorus between the atmosphere and the land surface. In terms of bioavailable phosphorus (which both the primary biogenic and biomass burning aerosols contain), a typical tropical forest net primary productivity (NPP) of approximately 1000 g m^{-2} yr^{-1} requires 0.6 g P m^{-2} yr^{-1} to maintain (tropical forests have on average 4116 moles C to 1 mole of

[25] Model results for the two cruises are shown in Figure 3. In order to determine whether these cruises are dominated by South American aerosols, we did an additional model simulation of only South American aerosols (not shown). These model results suggested that the cruise tracks in the tropical South Atlantic shown in Figure 3 are downwind of Africa (south of the equator) not the Amazon during October, when the observations were made. This is supported by back trajectories done for the JCR cruise [*Baker et al.*, 2005]. Because these cruises also suggest that primary biogenic particles or biomass burning aerosols are important sources of phosphorus, this suggests that the results we obtain in the Amazon in section 3.1 will be similar for other tropical forests. Note that model results show similar peaks and troughs, although the mineral aerosol component of phosphorus appears to be overestimated in model between 10°N–25°N and south of 35°N [*Hand et al.*, 2004].

4. Biogeochemical Implications

[26] Previous work in the Amazon and other lowland tropical regions has shown that changes in the phosphorus cycle can have substantial effects on several ecosystem processes, including primary productivity and decomposition [*Asner et al.*, 1999; *Townsend et al.*, 2002; *Cleveland et al.*, 2004; *Davidson et al.*, 2004]. As well, recent work from
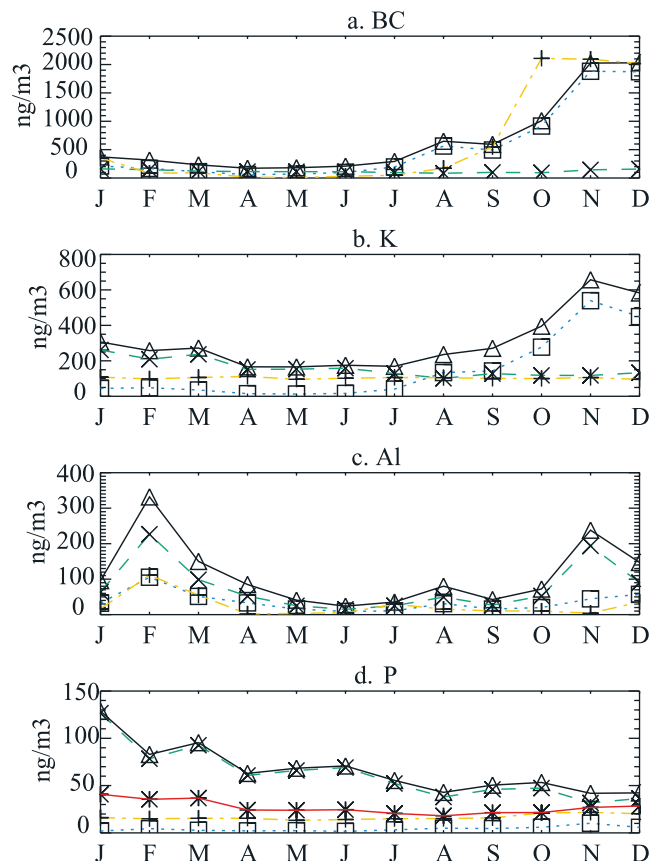

Figure 7. Same as Figure 4 but for Santarem.

Table 4. Estimated P Deposition at the Observational Sites, Including Estimates of Disturbed Deposition[a]

Site	Fine P, ng m^{-3}	Coarse P, ng m^{-3}	Fine P Deposition, mg m^{-2}yr^{-1}	Coarse P Deposition, mg m^{-2}yr^{-1}	Total Deposition, mg m^{-2}yr^{-1}	% Fine From Disturbed Sources	% Coarse From Disturbed Sources	Disturbed Deposition, mg m^{-2}yr^{-1}	% Deposition From Disturbed Sources	Pre-industrial Turnover Time	Disturbed Turnover Time
Alta Floresta	20.40	82.15	0.6	25.9	26.5	100.0	47.7	13.0	49.0	46	24
Balbina	4.95	29.81	0.2	9.4	9.6	58.7	7.2	0.8	8.0	71	66
Rondonia	4.69	24.57	0.1	7.7	7.9	100.0	21.7	1.8	23.2	103	79
Santarem	3.96	63.90	0.1	20.2	20.3	69.0	10.0	2.1	10.4	35	31
Average	**8.50**	**50.11**	**0.3**	**15.8**	**16.1**	**81.9**	**21.7**	**3.6**	**22.7**	**64**	**50**

[a]Assuming that the pre-industrial rate of biomass burning is 10% of contemporary values [*Wang and Jacob*, 1998]. This implies that disturbed sources are 90% of the biomass burning, and at Alta Floresta and Rondonia we assume also that 90% of the mineral aerosols come from disturbed sources. To estimate the disturbed deposition, we use our estimated disturbed aerosol concentration from Table 1 relative to the pre-industrial plus disturbed concentration we attribute to the sources (so we use only the fine and coarse contribution columns in Table 1 for this calculation). We assume dry deposition velocities of 0.1 and 1 cm s^{-1} for the fine and coarse mode respectively [*Seinfeld and Pandis*, 1996]. Pre-industrial and disturbed turnover times are relative to the 0.6 gP m^{-2} required to sustain 1000 gC m^{-2} NPP at these sites [*McGroddy et al.*, 2004].

P [*McGroddy et al.*, 2004]). Using the aerosol concentrations observed at Alta Floresta (20 and 82 ng P m^{-3} for the fine and coarse mode, respectively) and making simple assumptions of dry deposition velocities (0.1 and 1 cm s^{-1} for fine and coarse mode. respectively [from *Seinfeld and Pandis*, 1996], similar to our model dry deposition velocities), we obtain a gross deposition flux of 26 mg P m^{-2} yr^{-1}, or equivalently, that over ~24 years, all the phosphorus required for one year of forest growth is delivered from the atmosphere (see Table 4). It is difficult to determine the pre-industrial rate of biomass burning in the Amazon, and here we assume that that pre-industrial biomass burning emissions were 10% of contemporary levels similar to previous studies [e.g., *Wang and Jacob*, 1998]. Additionally, we assume that the Al at Alta Floresta (but not at other sites) comes from disturbed sources. With these assumptions, the pre-industrial turnover time of the phosphorus required for an NPP of approximately 1000 g m^{-2} yr^{-1} at Alta Floresta is 46 years (Table 4). Across the observational sites at the Amazon, deposition due to disturbed sources (defined as 90% of the biomass burning P and Alta Floresta P from Al) is approximately 23% of total deposition, suggesting an average shortening of the turnover time from 64 to 50 years from human disturbance.

[29] This estimate of a shortening of turnover time is necessarily sensitive to the assumptions used here, especially the pre-industrial rate of biomass burning. If we allow the estimates of turnover time to vary depending on the standard deviation in the P/BC, P/Al and P/K slopes shown in section 3.1, the turnover times are uncertain by <2 years. This is because the slopes have small uncertainties in them from a statistical standpoint. Uncertainties in the deposition rates or the amount of phosphorus required for the NPP will shift both the pre-industrial and current climate turnover times by a proportional factor. The real uncertainty in these estimates lie in the assumptions, and thus it is difficult to quantify them.

[30] To make basin-wide estimates of the impacts of phosphorus aerosols we use the model simulations described in sections 2.2 and 3.2 (Figure 8 and Table 5). Modeling of the phosphorus in mineral aerosols, biomass burning and primary biogenic particles suggests that over the Amazon, a substantial portion of the phosphorus will be

from biomass burning aerosols (Figure 8) and the net deposition of phosphorus is often negative, due to the local source to the atmosphere. Note the high spatial heterogeneity in phosphorus deposition shown in Figure 8, suggesting that disturbed and undisturbed regions may have quite different net balances of phosphorus. Additionally, note that both the observations and the model results clearly show the strong seasonality of aerosols in the Amazon, and the different seasonalities that occur in different regions of the Amazon. However, for terrestrial biogeochemistry, phosphorus inputs on longer time frames are important, and so for this section we focus on annually average source and deposition fields.

[31] Although data on phosphorus losses during biomass burning are relatively rare, the few in situ studies that do exist suggest that approximately 60% is lost from the ecosystem during and just after fire [*Pivello and Coutinho*, 1992; *Kauffman et al.*, 1994, 1995]. The loss of nitrogen and carbon tends to be much higher, which results in changes in the ratios of important nutrients due to fire, as discussed by *Hungate et al.* [2003]. Since there is approximately 600 μg P g C^{-1} in tropical forests [*McGroddy et al.*, 2004], our observed emissions ratio of 1–10 μg P g C^{-1} for biomass burning aerosols at our remote sampling sites suggests that there is substantial phosphorus from biomass burning that is not accounted for. In Figure 9 we speculate that the remaining phosphorus is lost in phosphorus bound to large ash particles (>100 μm) that are too large to be transported more than a few tens of km or observed at the measurement stations analyzed here. This effect has been suggested in previous studies of phosphorus at close to burned locations [e.g., *Diez et al.*, 1997] (reviewed by *Martinelli* [2003]). If we include the redistribution of phosphorus caused by ash particles within the Amazon Basin, deposition is 0.04 g P m^{-2} yr^{-1} (Table 5), meaning that all the P required for 1000 g C m^{-2} yr^{-1} NPP (0.6 g P) is deposited over a period of ~14 years. The biomass burning phosphorus associated with large ash particles may dominate the atmospheric phosphorus budgets in regions in close proximity to biomass burning.

[32] Globally, mineral aerosols constitute the largest source of aerosol phosphorus (not shown, but similar to *Graham and Duce* [1979] and *Okin et al.* [2004]), but over
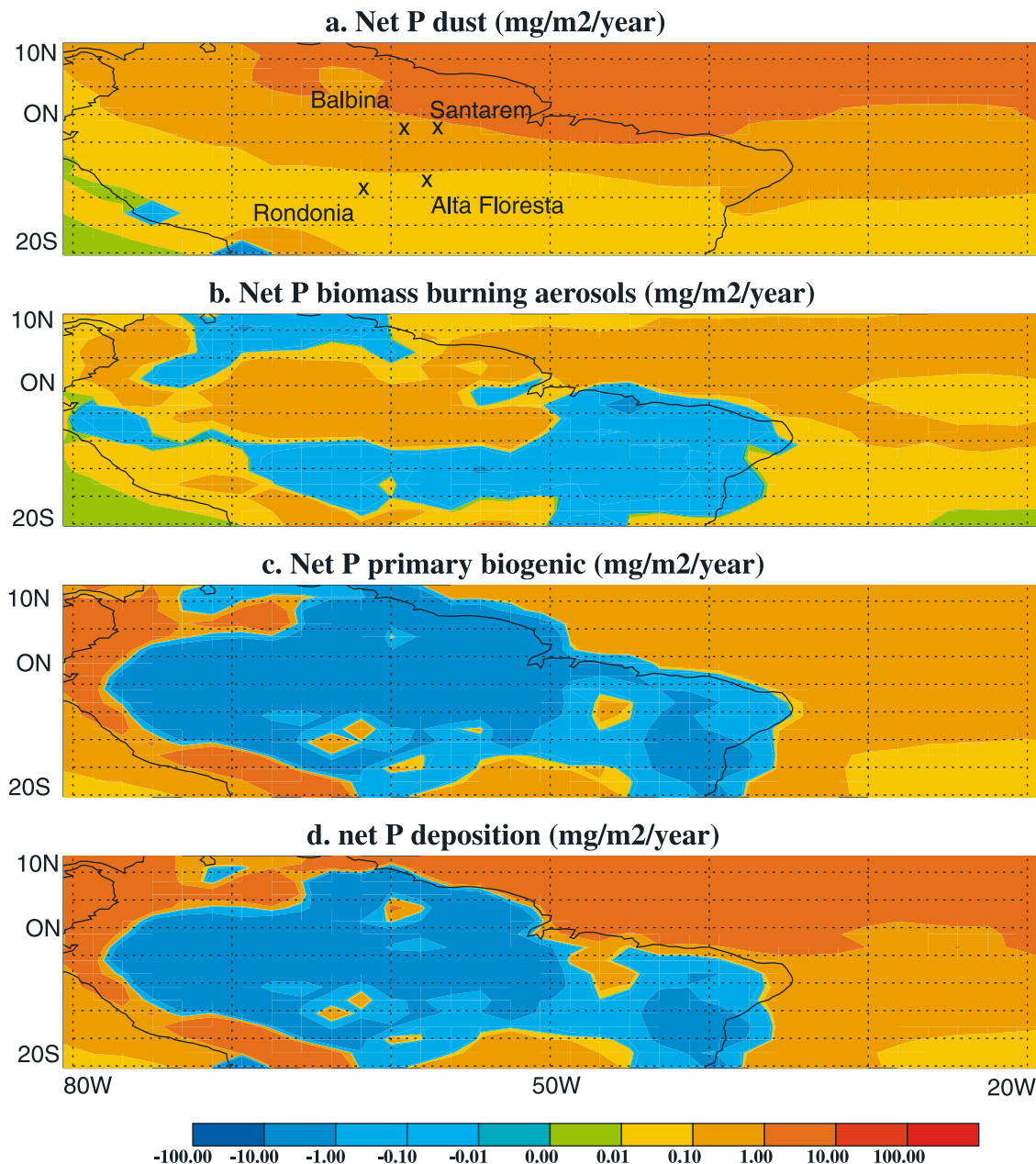
Figure 8. Model net deposition (deposition-source) of phosphorus from (a) mineral aerosols, (b) biomass burning, and (c) primary biogenic aerosols and (d) all aerosols net from model simulations described in sections 2.2 and 3.2. Also shown are the locations of the observing stations.

Table 5. Phosphorus Deposition From Postulated Sources From Model[a]

Phosphorus Source	Gross Amazon Deposition, mg m^{-2}yr^{-1}	Amazon Source, mg m^{-2}yr^{-1}	Net Deposition to Amazon (Deposition-Source), mg m^{-2}yr^{-1}	Relative Uncertainty
Mineral aerosols from natural sources	0.48	0.0	0.48	medium
Biomass burning fine aerosols	0.27	0.35	−0.08	high
Biomass burning coarse aerosols	0.41	0.48	−0.07	high
Primary biogenic aerosols	5.7	7.6	−1.9	very high
Net aerosol (fine plus coarse)	**6.9**	**8.5**	**−1.6**	
Biomass burning ash	43	43	0.0 (?)	very high

[a]Amazon: defined as land regions between 15°S to 5°N and 290°E to 330°E. We assume that there is 600 μg P g C^{-1} in the biomass burning ash [*McGroddy et al.*, 2004], with 60% of that released to the atmosphere in the form of ash [*Pivello and Coutinho*, 1992; *Kauffman et al.*, 1994, 1995].
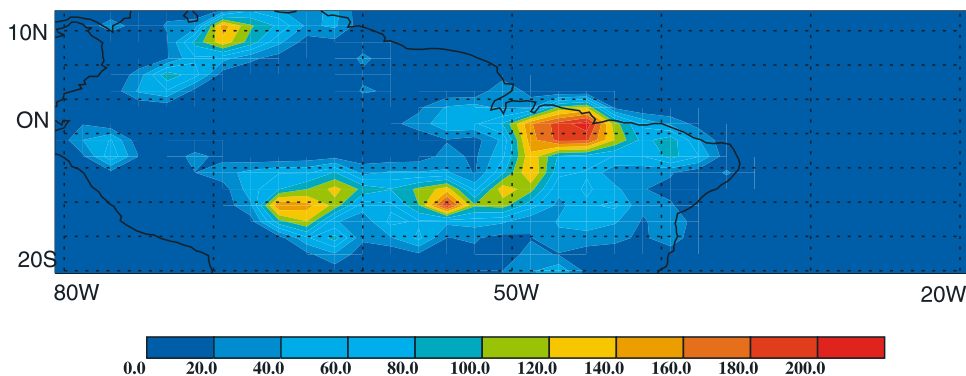
Figure 9. Ash phosphorus source and deposition, calculated from the biomass burning source [*van der Werf et al.*, 2003] assuming 600 μg P gC^{-1} ratios in the biomass burned [*McGroddy et al.*, 2004], and 60% phosphorus loss due to biomass burning [*Pivello and Coutinho*, 1992; *Kauffman et al.*, 1994, 1995]. Owing to the large size of the ash particles, we assume that the ash is redeposited in the same grid box as emitted.

the Amazon (defined as land regions between $15°S$ to $5°N$ and $290°E$ to $330°E$), the deposition of phosphorus from biomass burning emissions or primary biogenic aerosols is large, as evidenced by the domination of phosphorus from these aerosols (section 3.1). Using the modeled aerosol deposition for the entire basin (where the model underestimates phosphorus by a factor of 2 compared to the observations as seen in Figure 2), the gross deposition rate of phosphorus in the basin is 6.9 mg P m^{-2} yr^{-1}, indicating that all the phosphorus required for 1000 gC m^{-2} NPP is cycled through the atmosphere over the entire basin every 90 years. Although human land use change and biomass burning is leading to substantial increases in the deposition of phosphorus in undisturbed areas within the Amazon Basin, on the whole, atmospheric transport is leading to a net loss of phosphorus (Table 5). In net terms, phosphorus is estimated to be leaving the Amazon through the atmosphere at a rate of 1.3 mg P m^{-2} yr^{-1} (Table 5). This loss rate of phosphorus is equivalent to losing the phosphorus required for current levels of NPP over ∼380 years over the entire Amazon basin (although phosphorus in soil pools may become more available [*Lloyd et al.*, 2001]). Approximately 50% of the observed phosphorus over the Alta Floresta site appears to be linked with human activity (Table 4). Thus the potential of remaining undisturbed tropical forests to serve as a carbon sink may be enhanced via this mechanism over the next several decades [*Davidson et al.*, 2004]. However, in the long term, slow leakage of phosphorus through the atmosphere will occur, reducing soil fertility and ecosystem productivity [*Wardle et al.*, 2004]. On a wider scale, these human-linked emissions may also serve to fertilize areas of the ocean where phosphorus is limiting [e.g., *Mills et al.*, 2004].

References

Andreae, M. O. (1983), Soot carbon and excess fine potassium: Long-range transport of combustion-derived aerosols, *Science*, *220*, 1148–1151.

Andreae, M. O., and P. Merlet (2001), Emission of trace gases and aerosols from biomass burning, *Global Biogeochem. Cycles*, *15*(4), 955–966.

Andreae, M. O., et al. (1998), Airborne studies of aerosol emissions from savanna fires in southern Africa: 2. Aerosol chemical composition, *J. Geophys. Res.*, *103*(D24), 32,119–32,128.

Artaxo, P., and W. Maenhaut (1990), Aerosol characteristics and sources for the Amazon Basin during the west season, *J. Geophys. Res.*, *95*(D10), 16,971–16,985.

Artaxo, P., and C. Orsini (1987), PIXE and receptor models applied to remote aerosol source apportionment in Brazil, *Nucl. Instrum. Methods Phys. Res., Sect. B*, *22*, 259–263.

Artaxo, P., H. Storms, F. Bruynseels, R. V. Greiken, and W. Maenhaut (1988), Composition and sources of aerosols from the Amazon Basin, *J. Geophys. Res.*, *93*(D2), 1605–1615.

Artaxo, P., E. Fernandes, J. Martins, M. Yamasoe, P. Hobbs, W. Maenhaut, K. Longo, and A. Castanho (1998), Large-scale aerosol source apportionment in Amazonia, *J. Geophys. Res.*, *103*, 31,837–31,847.

Artaxo, P., J. V. Martins, M. A. Yamasoe, A. S. Procopio, T. M. Pauliquevis, M. O. Andreae, P. Guyon, L. V. Gatti, and A. M. C. Leal (2002), Physical and chemical properties of aerosols in the wet and dry seasons in Rondonia, Amazonia, *J. Geophys. Res.*, *107*(D20), 8081, doi:10.1029/2001JD000666.

Asner, G. P., A. R. Townsend, and M. C. Bustamante (1999), Spectrometry of pasture condition and biogeochemistry in the central Amazon, *Geophys. Res. Lett.*, *26*, 2769–2772.

Baker, A. R. (2004), Inorganic iodine speciation in tropical Atlantic aerosol, *Geophys. Res. Lett.*, *31*, L23S02, doi:10.1029/2004GL020144.

Baker, A. R., S. D. Kelly, K. F. Biswas, M. Witt, and T. D. Jickells (2003), Atmospheric deposition of nutrients to the Atlantic Ocean, *Geophys. Res. Lett.*, *30*(24), 2296, doi:10.1029/2003GL018518.

Baker, A. R., T. D. Jickells, M. Witt, and K. L. Linge (2005), Trends in the solubility of iron, aluminium, manganese and phosphorus in aerosol collected over the Atlantic Ocean, *Mar. Chem.*, in press.

Cachier, H., C. Liousse, P. Buat-Menard, and A. Gaudichet (1995), Particulate content of savanna fire emissions, *J. Atmos. Chem.*, *22*, 123–148.

Chadwick, O. A., L. A. Derry, P. M. Vitousek, B. J. Huebert, and L. O. Hedin (1999), Changing sources of nutrients during four million years of ecosystem development, *Nature*, *397*, 491–496.

Chen, M., P. Xie, J. Janowiak, and P. Arkin (2002), Global land precipitation: A 50-year monthly analysis based on gauge data, *J. Hydrometeorol.*, *3*(3), 249–266.

Clark, D. A. (2002), Are tropical forests an important carbon sink? Reanalysis of the long-term plot data, *Ecol. Appl.*, *12*(1), 3–7.

Cleveland, C. C., A. R. Townsend, S. K. Schmidt, and B. C. Constance (2004), Soil microbial dynamics and biogeochemistry in tropical forests and pastures, *Ecol. Appl.*, *13*(2), 314–326.

Davidson, E. A., C. Carvalho, I. Viera, R. Figueriedo, P. Moutinho, F. Ishida, M. Santos, J. Guerrero, K. Kalif, and R. Saba (2004),

Nutrient limitation of biomass growth in a tropical secondary forest: Early results of a nitrogen and phosphorus amendment experiment, *Ecol. Appl.*, *14*(4), S150–S163.

Dickinson, R., and A. Henderson-Sellers (1988), Modeling tropical deforestation—A study of GCM land surface parameterizations, *Q. J. R. Meteorol. Soc.*, *114*(480), 439–462.

Diez, J., A. Polo, M. Diaz-Burgos, C. Cerri, B. Feigl, and M. Piccolo (1997), Effect of fallow land, cultivated pasture and abandoned pasture on soil fertility in two deforested Amazonian regions, *Sci. Agricola*, *54*(1–2), 1–13.

Echalar, F., A. Guadichet, H. Cachier, and P. Artaxo (1995), Aerosol emissions by tropical forest and savanna biomass burning: Characteristic trace elements and fluxes, *Geophys. Res. Lett.*, *22*(22), 3039–3042.

Fecan, F., B. Marticorena, and G. Bergametti (1999), Parameterization of the increase of the Aeolian erosion threshold wind friction velocity due to soil moisture for arid and semi-arid area, *Ann. Geophys.*, *17*, 149–157.

Ferek, R., J. Reid, P. Hobbs, D. Blake, and C. Liousse (1998), Emission factors of hydrocarbons, halocarbons, trace gases and particles from biomass burning in Brazil, *J. Geophys. Res.*, *103*(D24), 32,107–32,118.

Field, C. B., M. J. Behrenfeld, J. T. Randerson, and P. Falkowski (1998), Primary production of the biosphere: Integrating terrestrial and oceanic component, *Science*, *281*, 237–240.

Gaudichet, A., F. Echalar, B. Chatenet, J. P. Quisefit, G. Malingre, H. Cachier, P. Buat-Menard, P. Artaxo, and W. Maenhaut (1995), Trace elements in tropical African savanna biomass burning aerosols, *J. Atmos. Chem.*, *22*, 19–39.

Gillette, D. A., E. Hardebeck, and J. Parker (1997), Large-scale variability of wind erosion mass flux rates at Owens Lake: 2. Role of roughness change, particle limitation, change of threshold friction velocity, and the Qwen effect, *J. Geophys. Res.*, *102*(D22), 25,989–25,998.

Ginoux, P., M. Chin, I. Tegen, J. Prospero, B. Holben, O. Dubovik, and S. J. Lin (2001), Sources and distributions of dust aerosols simulated with the GOCART model, *J. Geophys. Res.*, *106*(D17), 20,255–20,273.

Graham, B., et al. (2003), Composition and diurnal variability of the natural Amazonian aerosol, *J. Geophys. Res.*, *108*(D24), 4765, doi:10.1029/2003JD004049.

Graham, W. F., and R. A. Duce (1979), Atmospheric pathways of the phosphorus cycle, *Geochim. Cosmochim. Acta*, *43*, 1195–1208.

Graham, W. F., and R. A. Duce (1982), The atmospheric transport of phosphorus to the western North Atlantic, *Atmos. Environ.*, *16*(5), 1089–1097.

Hand, J., N. Mahowald, Y. Chen, R. Siefert, C. Luo, A. Subramaniam, and I. Fung (2004), Estimates of soluble iron from observations and a global mineral aerosol model: Biogeochemical implications, *J. Geophys. Res.*, *109*, D17205, doi:10.1029/2004JD004574.

Hungate, B., R. Naiman, M. Apps, J. Cole, B. Moldan, K. Satake, J. Stewart, R. Victoria, and P. Vitousek (2003), Disturbance and Elemental Interactions, in *Interactions of the Major Biogeochemical Cycles: Global Change and Human Impacts*, edited by J. Melillo, C. Field, and B. Moldan, pp. 47–62, Island Press, Washington, D. C.

Iversen, J. D., and B. R. White (1982), Saltation threshold on Earth, Mars and Venus, *Sedimentology*, *29*, 111–119.

Johansson, S., et al. (1995), *Particle-Induced X-Ray Emission Spectrometery (PIXE)*, John Wiley, Hoboken, N. J.

Kauffman, J. B., D. L. Cummings, and D. E. Ward (1994), Relationships of fire, biomass and nutrient dynamics along a vegetation gradient in the Brazilian cerrado, *J. Ecol.*, *82*(3), 519–531.

Kauffman, J. B., D. L. Cummings, D. E. Ward, and R. Babbitt (1995), Fire in the Brazilian Amazon: 1. Biomass, nutrient pools, and losses in slashed primary forests, *Oecologia*, *104*, 397–408.

Kistler, R., et al. (2001), The NCEP-NCAR 50-Year Reanalysis: Monthly means CD-ROM and documentation, *Bull. Am. Meteorol. Soc.*, *82*(2), 247–267.

Lloyd, J., M. I. Bird, E. M. Veenendaal, and B. Kruijt (2001), Should phosphorus availability be constraining moist tropical forest responses to increasing CO$_2$ concentrations?, in *Global Biogeochemical Cycles in the Climate System*, edited by E.-D. Schulze et al., pp. 95–114, Elsevier, New York.

Losno, R., G. Bergametti, and P. Carlier (1992), Origins of atmospheric particulate matter over the North Sea and the Atlantic Ocean, *J. Atmos. Chem.*, *15*, 333–352.

Luo, C., N. Mahowald, and J. del Corral (2003), Sensitivity study of meteorological parameters on mineral aerosol mobilization, transport, and distribution, *J. Geophys. Res.*, *108*(D15), 4447, doi:10.1029/2003JD003483.

Maenhaut, W., I. Salma, J. Cafmeyer, H. Annegard, and M. Andreae (1996), Regional atmospheric aerosol composition and sources in the eastern Transvaal, South Africa and impact of biomass burning, *J. Geophys. Res.*, *101*(D19), 23,631–23,650.

Mahowald, N., P. Rasch, B. Eaton, S. Whittlestone, and R. Prinn (1997), Transport of ^{222}radon to the remote troposphere using MATCH and assimilated winds from ECMWF and NCEP/NCAR, *J. Geophys. Res.*, *102*(D23), 28,139–28,152.

Mahowald, N., C. Zender, C. Luo, J. del Corral, D. Savoie, and O. Torres (2002), Understanding the 30-year Barbados desert dust record, *J. Geophys. Res.*, *107*(D21), 4561, doi:10.1029/2002JD002097.

Mahowald, N., C. Luo, J. del Corral, and C. Zender (2003), Interannual variability in atmospheric mineral aerosols from a 22-year model simulation and observational data, *J. Geophys. Res.*, *108*(D12), 4352, doi:10.1029/2002JD002821.

Malhi, Y., and J. Grace (2000), Tropical forests and atmospheric carbon dioxide, *Trends Ecol. Evol.*, *15*(8), 332–337.

Marticorena, B., and G. Bergametti (1995), Modeling the atmospheric dust cycle: 1. Design of a soil-derived dust emission scheme, *J. Geophys. Res.*, *100*(D8), 16,415–16,430.

Martinelli, L. (2003), Elemental interactions in Brazilian landscapes as influenced by human interventions, in *Interactions of the Major Biogeochemical Cycles: Global Change and Human Impacts*, edited by J. Melillo, C. Field, and B. Moldan, pp. 193–210, Island Press, Washington, D. C.

Martinelli, L., et al. (1999), Nitrogen stable isotopic composition of leaves and soil: Tropical versus temperate forests, *Biogeochemistry*, *46*(1–3), 45–65.

Martins, J., P. Artaxo, C. Liousse, J. Reid, P. Hobbs, and Y. Kaufman (1998a), Effects of black carbon content, particle size and mixing on light absorption by aerosol particles from biomass burning in Brazil, *J. Geophys. Res.*, *103*(D24), 32,041–32,050.

Martins, J., P. Hobbs, R. Weiss, and P. Artaxo (1998b), Morphology and structure of smoke particles from biomass burning in Brazil, *J. Geophys. Res.*, *103*(D24), 32,051–32,058.

Mason, B., and C. Moore (1984), *Principles of Geochemistry*, 4th ed., John Wiley, Hoboken, N. J.

McGroddy, M., T. Daufresne, and L. Hedin (2004), Scaling of C:N:P stoichiometry in forests worldwide: Implications of terrestrial Redfield-type ratios, *Ecology*, *85*(9), 2390–2401.

Mills, M. M., C. Ridame, M. Davey, J. LaRoche, and R. Geider (2004), Iron and phosphorus co-limit nitrogen fixation in the eastern tropical North Atlantic, *Nature*, *429*, 292–294.

Okin, G., N. Mahowald, O. Chadwick, and P. Artaxo (2004), The impact of desert dust on the biogeochemistry of phosphorus in terrestrial ecosystems, *Global Biogeochem. Cycles*, *18*, GB2005, doi:10.1029/2003GB002145.

Penner, J. E., et al. (2001), Aerosols, their direct and indirect effects, in *Climate Change 2001: The Scientific Basis*, edited by J. T. Houghton et. al., pp. 289–348, Cambridge Univ. Press, New York.

Pivello, V. R., and L. M. Coutinho (1992), Transfer of macronutrients to the atmosphere during experimental burnings in an open cerrado (Brazilian savanna), *J. Trop. Ecol.*, *8*, 487–497.

Pye, K. (1987), *Aeolian Dust and Dust Deposits*, 334 pp., Elsevier, New York.

Rasch, P. J., N. M. Mahowald, and B. E. Eaton (1997), Representations of transport, convection and the hydrologic cycle in chemical transport models: Implications for the modeling of short-lived and soluble species, *J. Geophys. Res.*, *102*(D23), 28,127–28,138.

Rasch, P. J., W. Collins, and B. E. Eaton (2001), Understanding the Indian Ocean Experiment (INDOEX) aerosol distributions with an aerosol assimilation, *J. Geophys. Res.*, *106*(D7), 7337–7355.

Reid, J., P. Hobbs, R. Ferek, D. Blake, J. Martins, M. Dunlap, and C. Liousse (1998), Physical, chemical and optical properties of regional hazes dominated by smoke in Brazil, *J. Geophys. Res.*, *103*(D24), 32,059–32,080.

Sanchez, P., D. Bandy, J. Villachica, and J. Nicholaides (1982), Amazon Basin soils: Management for continuous crop production, *Science*, *216*, 812–827.

Seinfeld, J., and S. Pandis (1996), *Atmospheric Chemistry and Physics: From Air Pollution to Climate Change*, John Wiley, Hoboken, N. J.

Shukla, J., C. Nobre, and P. Sellers (1990), Amazon deforestation and climate change, *Science*, *247*, 1322–1325.

Swap, R., et al. (1992), Saharan dust in the Amazon Basin, *Tellus, Ser. B*, *44*, 133–149.

Townsend, A. R., P. M. Vitousek, and E. A. Holland (1992), Tropical soils could dominate the short-term carbon cycle feedbacks to increased global temperatures, *Clim. Change*, *22*(4), 293–303.

Townsend, A., G. P. Asner, C. C. Cleveland, M. E. Lefer, and M. Bustamante (2002), Unexpected changes in soil phosphorus dynamics along pasture chronosequences in the humid tropics, *J. Geophys. Res.*, *107*(D20), 8067, doi:10.1029/2001JD000650.

Turn, S., B. Jenkins, J. Chow, L. Pritchett, D. Campbell, T. Cahill, and S. Whalen (1997), Elemental characterization of particulate matter emitted from biomass burning: Wind tunnel derived source profiles for herbaceous and wood fuels, *J. Geophys. Res.*, *102*(D3), 3633–3699.

van der Werf, G. R., J. T. Randerson, G. J. Collatz, and L. Giglio (2003), Carbon emissions from fires in tropical and subtropical ecosystems, *Global Change Biol.*, *9*, 547–562.

Vitousek, P. (1984), Litterfall, nutrient cycling and nutrient limitations in tropical forests, *Ecology*, *65*(1), 285–298.

Vitousek, P. M., T. Fahey, D. W. Johnson, and M. J. Swift (1988), Element interactions in forest ecosystems—Succession, allometry and input-output budgets, *Biogeochemistry*, *5*(1), 7–34.

Wang, Y., and D. Jacob (1998), Anthropogenic forcing on tropospheric ozone and OH since pre-industrial times, *J. Geophys. Res.*, *103*(D23), 31,123–31,135.

Wardle, D., L. R. Walker, and R. D. Bardgett (2004), Ecosystem properties and forest decline in contrasting long-term chronosequences, *Science*, *305*, 509–513.

Zender, C., H. Bian, and D. Newman (2003), The mineral dust entrainment and deposition model DEAD: Description and 1990s dust climatology, *J. Geophys. Res.*, *108*(D14), 4416, doi:10.1029/2002JD002775.

————————————

P. Artaxo, Instituto de Fisca, Universidade de Sao Paulo, Rua do Matao, Travessa R., 197, CEP 05508-900, Sao Paulo, S.P., Brazil. (artaxo@if.usp.br)

A. R. Baker and T. D. Jickells, School of Environmental Sciences, University of East Anglia, Norwich, NR4 7TJ, UK. (alex.baker@uea.ac.uk; t.jickells@uca.ac.uk)

N. M. Mahowald, National Center for Atmospheric Research, Boulder, CO 80307, USA. (mahowald@ucar.edu)

G. S. Okin, Department of Environmental Sciences, University of Virginia, P. O. Box 400123, 291 McCormick Road, Charlottesville, VA 22904-4123, USA. (okin@virginia.edu)

J. T. Randerson, Earth System Science Department, University of California, 3212 Croul Hall, Irvine, CA 92697-3100, USA. (jranders@uci.edu)

A. R. Townsend, Department of Ecology and Evolutionary Biology and Institute of Arctic and Alpine Research, University of Colorado, Boulder, CO 80309, USA. (townsena@colorado.edu)